*Iraqi Journal of Physics, 2025*
*https://doi.org/10.30723/ijp.v23i2.1366*

*Vol. 23, No.2, PP. 80-88*
*P-ISSN: 2070-4003*
*E-ISSN: 2664-5548*

# Influence of pH on the Photocatalytic Activity of $Ag/Fe_2O_3$ and $S/Fe_2O_3$ Nanoparticles by Methyl Blue Dye Degradation

**Baraa Aqeel Kaerrm[1*] and Ban Mazin Alshabander[1]**
[1]*Department of Physics, College of Science, University of Baghdad, Baghdad, Iraq*
[b]E-mail: ban.muzahem@sc.uobaghdad.edu.iq
[a*]Corresponding author: baraa.aqeel2304@sc.uobaghdad.edu.iq

## Abstract

In this research, iron oxide ($Fe_2O_3$) nanoparticles were doped with 5% mol of metallic material silver (Ag) and non-metallic material sulfur (S) by a wet impregnation process. Scanning electron microscopy (SEM) was used to determine the shape and arrangement of the crystals. UV-Vis spectroscopy was used to study the photocatalytic degradation of dye pollutants by measuring the absorbance spectra of the $Ag/Fe_2O_3$ and $S/Fe_2O_3$ nanoparticle samples. The objective of this study was to investigate the impact of pH on the photocatalytic activity of nanoparticles. The pH of a 5ppm solution of methylene blue (MB) dye was changed to 3 and 8 using hydrochloric acid (HCl) and sodium hydroxide (NaOH). In pH=8, $Ag/Fe_2O_3$ takes 240 min to reach nearly 93.35% degradation, while $S/Fe_2O_3$ achieves over 90% degradation in the first 60 min of the photocatalysis process. At pH=3, $Ag/Fe_2O_3$ achieves only 34.46 %, while $S/Fe_2O_3$ achieves 61.44% decomposition after 240 min. The pseudo-first-order kinetic model was found to be the best fit for the adsorption of MB by the two catalysts.

**Article Info.**

**Keywords:**
*$Fe_2O_3$, Photo Catalysts, Methyl Blue (MB), Dye, Degradation.*

**Article history:**
*Received: Oct.04, 2024*
*Revised: Dec. 23, 2024*
*Accepted:Dec.29, 2024*
*Published:Jun.01,2025*

## 1. Introduction

The textile, paper, leather, food, plastic, and cosmetics industries produce toxic dyes in water streams, which greatly contribute to environmental pollution. These dyes have the potential to contaminate river water [1-3]. Therefore, it is essential to manage it efficiently prior to releasing it directly into water bodies or onto uncovered land. Wastewater can be treated using various techniques, such as physical (heat treatment) (filtration), chemical (sorption), biological (disinfection) processes and catalytic oxidation were designed and used for the degradation of the contaminant [4]. Photocatalytic degradation is considered one of the most successful methods for eliminating dyes from wastewater, among many physical and chemical treatments [5]. Photocatalysis is the process of utilizing light to initiate or expedite chemical reactions by altering the characteristics of compounds known as photocatalysts [6].

Metal oxide semiconductors, such as $TiO_2$, ZnO, $WO_3$, $Fe_2O_3$, etc., have shown to possess good photocatalytic activity toward the degradation of toxic organic pollutants into nontoxic molecules, such as $CO_2$ and $H_2O$, under illumination of light [7]. Hematite ($Fe_2O_3$) stands out among metal oxides due to its exceptional stability, affordability, strong oxidative capabilities, environmental compatibility, and ability to harvest visible light—qualities that make it an excellent candidate for a wide range of catalytic applications. However, the low band gap energy (2.2-2.4 eV) and the high recombination rate of electron-hole pairs in hematite limit its effectiveness in photocatalytic applications [8]. To enhance its performance of photocatalytic activity, various strategies have been explored, including architectural control, quantum confinement, and hetero-atom doping, among others [9-12]. Chemical methods, including hetero-atom doping or composite semiconductors, can be used to improve its performance. This promotes charge transfer by improving the electronic structures and optical properties of $Fe_2O_3$.

Metal doping, with Ag, Zn, Sn, Cu, Zr, Co, Mn, Pb or Si, could be beneficial for the Photoelectrochemical Cell (PEC) properties of the hematite photoelectrode especially its conductivity and charge transport [13-15]. Nonmetal doping with N, S, and P has also proved beneficial in different materials, including hematite. It has been shown that the bandgap can be tenable by making the 2p orbital of the oxygen be hybridized due to the non-metallic doping [16-19].

In this study, Ag/$Fe_2O_3$, S/$Fe_2O_3$ doped hematite nanoparticles were prepared using the impregnation method. To confirm the advantages of doping hematite with Ag and S, the materials prepared were characterized by SEM analysis and evaluated for their effectiveness in the degradation of methylene blue (MB) through adsorption and photocatalytic processes. Additionally, the effects of pH at 3, 7, and 8 on the photocatalytic processes were investigated.

## 2. Experimental Part

### 2.1. Materials

Iron oxide ($Fe_2O_3$) was purchased from Sky Spring Nanomaterials, Inc., with a particle size range of 20–40 nm and a purity of >99%. Silver nitrate ($AgNO_3$) and sodium sulfide ($Na_2SO_4$) were used as sources of Ag and S, respectively, and were purchased from Fisher Certified Company with extra purity. The azo dye, methyl blue (MB, $C_{16}H_{18}ClN_3S$), sodium hydroxide (NaOH) with >98% purity, and hydrochloric acid (HCl) with 36% purity were supplied by Sigma-Aldrich.

### 2. 2. Preparation of Metal Doped $Fe_2O_3$ (Ag) and Non-Metal Doped $Fe_2O_3$ (S) Nanoparticles

Ag/$Fe_2O_3$ and S/$Fe_2O_3$ photocatalysts were prepared using the impregnation technique. $AgNO_3$ and $Na_2SO_4$ were used as a source of Ag and S nanoclusters, respectively, which are crafted on the surface of $Fe_2O_3$ as stated earlier [20]. A 5-molarity ratio of $AgNO_3$ or $Na_2SO_4$ with 1 g of $Fe_2O_3$ nanoparticles was added to 20 mL of distilled water. In order to obtain a uniformly blended solution, the solution was vigorously mixed by magnetic stirrers at a speed of 1500 rpm and a temperature of 90 °C for 60 min. Then, it was necessary to let the combination rest for 15 min at room temperature; after that, the materials were washed twice with distilled water to remove any impurities or contaminants. To evaporate water, drying process was done in an oven at 110 °C for 2 hrs. The colour of Ag/ $Fe_2O_3$ and S/ $Fe_2O_3$ nanoparticles changed from red to brown. An agate mortar was used to grind the Ag/ $Fe_2O_3$ or S/ $Fe_2O_3$ nanoparticles until it became a fine powder. All steps of the experimental work are illustrated in Fig.1.

### 2. 3. Photocatalytic Activity

The photocatalytic activity of the nanocomposite samples, consisting of the Ag/$Fe_2O_3$ and S/$Fe_2O_3$, was studied by examining the photo degradation of an aqueous solution of MB dye under sunlight irradiation with an intensity of about 416 – 833 W/$m^2$ from 10.00 am to 2.00 pm at temperature (25-30) °C. 10 mg of photocatalyst was put in a 40 ml of MB solution at 5ppm concentration in darkness for 60 min to achieve an equilibrium between the adsorption and desorption of MB on the photocatalysts surface. The degradation of MB through exposure to light was quantified by measuring the absorbance of solutions using a spectrophotometer. Distilled water was used as a reference to MB solutions. The effectiveness of photodegradation was determined by calculating the absorption intensity at a wavelength of 664 nm. The following equation was used to determine the photodegradation efficiency of MB dye [21]

$$\text{DEGRADATION}\,\% = \frac{A_0 - A_T}{A_0} \times 100\% \qquad (1)$$

where $A_0$ and $A_t$ are the initial and the final absorbance after irradiation process, respectively.

$$\text{Ln}\frac{A_0}{A_t} = kt \qquad (2)$$

where k is the photodegradation rate constant (min $^{-1}$) [21, 22].

To study the effect of pH on the degradation of pollutants, the pH of the MB solution was varied from 3 to 8 using (0.1 N) HCl and (0.1N) NaOH. After dilution, drops of HCL or NaOH were added after dilution to the solution containing MB to examine the effect of acidity and basicity on photocatalysis.

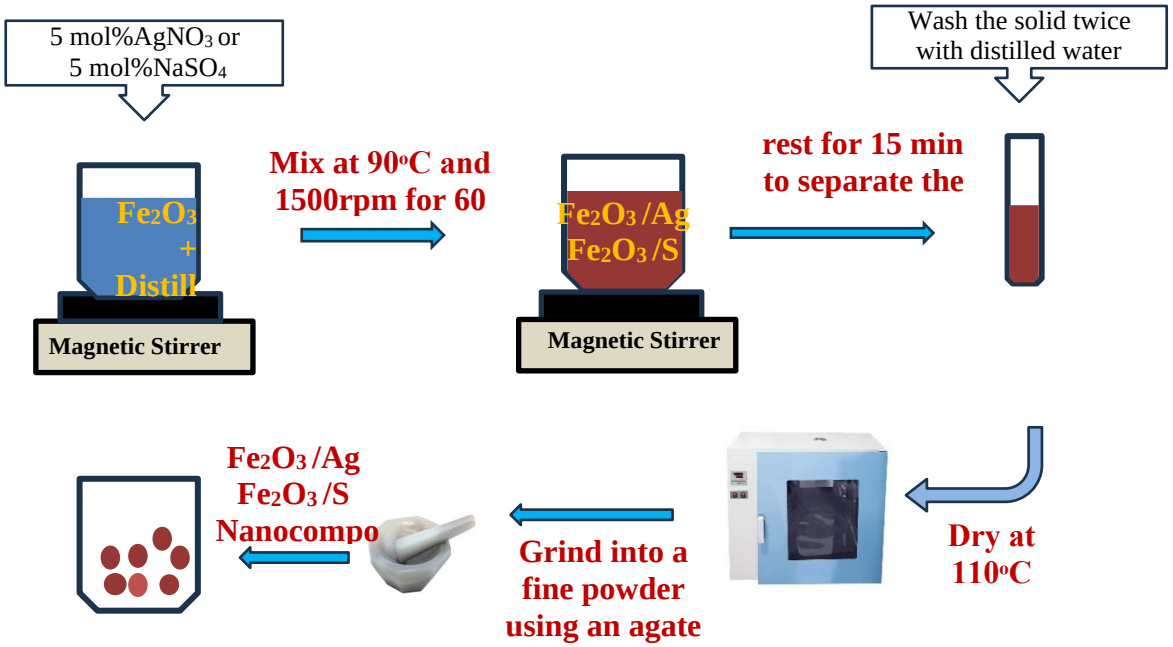


***Figure 1: Preparation method diagram of Ag/ $Fe_2O_3$ and S/ $Fe_2O_3$ nanoparticles samples.***

### 2. 4. Characterization

Scanning Electron Microscopy (SEM) is an analytical technique widely used to study the topography, texture and surface features of powders. The SEM produces a 3D view of a specimen, which is important to examine the shape and structure of a specimen. SEM (Model JEOL-JSM-6360, Japan) was employed to analyses the morphology of Ag/$Fe_2O_3$ and S/$Fe_2O_3$ samples with enhanced resolution, depth of field, and magnification. UV-visible spectrophotometer (SHIMADZU: UV-1800) was used to analyse the photocatalytic degradation of dye pollutants by measuring the absorbance spectra of the Ag/$Fe_2O_3$ and S/$Fe_2O_3$ samples.

## 3. Results and Discussion

### 3. 1. Scanning Electron Microscopy Studies

A scanning electron microscope was used to check the morphology of the prepared samples. Fig. 2 (a) illustrates an SEM image of Ag/$Fe_2O_3$, indicating that the sample has great homogeneity and well-defined forms. The tetragonal form of the produced Ag/$Fe_2O_3$ NPs with a dimension of about 24.26 nm was noticed. Surface roughness is significant in improving photocatalytic properties. The nanoparticles of S/$Fe_2O_3$ were seen

in the SEM image (Fig. 2 (b)) to be of no definite shape, but some particles possess spherical morphology. The diameters of the particles were about 26.53nm.

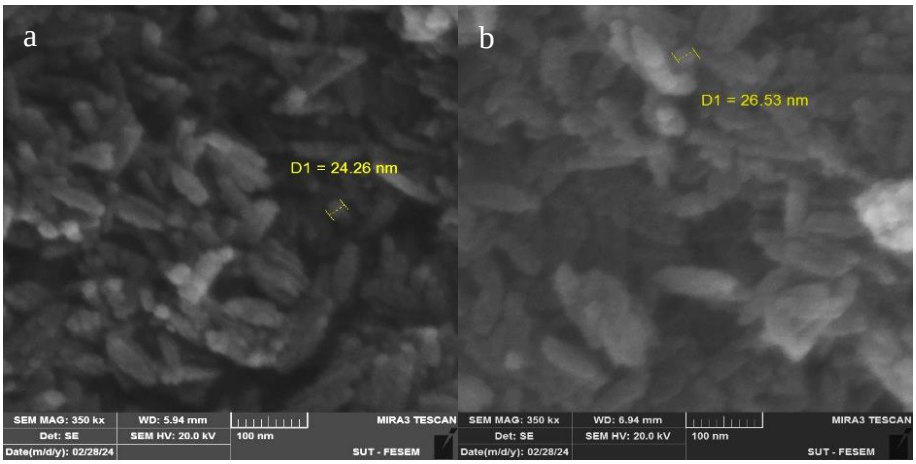


***Figure 2: SEM images of Ag /$Fe_2O_3$ and S/$Fe_2O_3$ nanoparticles samples.***

### 3. 2. Photocatalyst Activity of Ag/$Fe_2O_3$ and S/$Fe_2O_3$ Nanoparticles

Methyl blue (MB) dye was used as a model of organic pollutants to examine the ability of Ag/$Fe_2O_3$ and S/$Fe_2O_3$ nanoparticles to water purification treatment under sunlight. Figs. 3 and 4 show the changes in the absorption of MB solution over time for Ag/$Fe_2O_3$ and S/$Fe_2O_3$ nanoparticles at three pH values (3, 7 and 8) at different irradiation times. It is clear from these figures that pH=8, which is alkaline conditions, shows the best Photocatalyst activity for faster and more efficient degradation of MB solutions than at pH=3, which is acidic conditions, over the same period.

Hydroxyl groups (•OH)are a functional group associated with $Fe_2O_3$.The surface (•OH) groups may be arranged to one, two or three underlying iron atoms. The overall density of hydroxyl groups depends on the crystal structure and faces.

The surface charge of oxides is determined by the adsorption or desorption of protons, which varies with the pH of the surrounding solution [23]. The isoelectric point, corresponding to the pristine point of zero charge (PZC), is approximately pH 8.5 for materials of various shapes. Below this pH, $FeOH_2^+$ groups dominate, resulting in an overall positive surface charge. In contrast, at pH values above the PZC, the fraction of negatively charged $FeO^-$ groups increases. Zeta potential studies revealed that the point of zero charge was at pH=6.8 and pH=8.5 for the $Fe_2O_3$ nanoparticles [24].

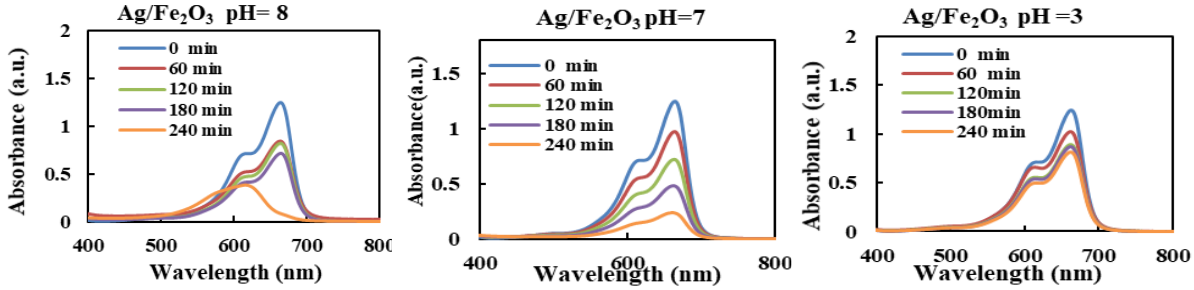


***Figure 3: UV-Vis absorption spectra of MB (5ppm) catalysis by Ag/$Fe_2O_3$ nanoparticles at pH= 8, pH=7 & pH=3 at different irradiation times (0-240 min) under sunlight irradiation.***

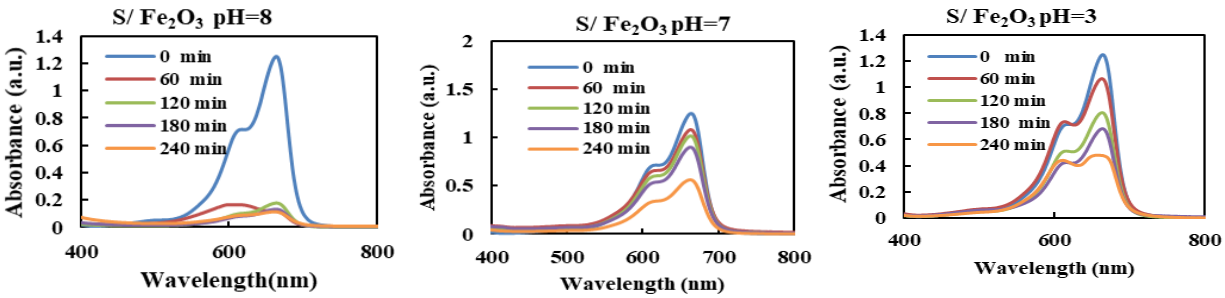


***Figure 4: UV-Vis absorption spectra of MB (5ppm) catalysis by S/$Fe_2O_3$ nanoparticles at pH= 8, pH=7 & pH=3 at different irradiation times.***

The pH of the solution is a crucial determinant in the process of photocatalytic degradation. It has been observed that the pH level significantly impacts the adsorption of dyes onto the surface of $Fe_2O_3$ nanoparticles. At a high pH, there may be an increased abundance of hydroxyl ions, which can react with hydrogen ions to generate OH-. This, in turn, accelerates the degradation of dyes [17, 25, 26]. Fig.5 presents the degradation rate (D%) of the two samples, Ag/$Fe_2O_3$ and S/$Fe_2O_3$**,** against different irradiation times for different values of pH.

S/$Fe_2O_3$ surpass Ag/$Fe_2O_3$ in all pH=8, pH=7 and pH=3 environments. In pH=8, Ag/$Fe_2O_3$ takes 240 min to reach nearly 93.35%, while S/$Fe_2O_3$ achieves over 90% degradation in the first 60 min of the photocatalysis process. At pH=3, Ag/$Fe_2O_3$ achieves only 34.46 %, while S/$Fe_2O_3$ achieves 61.44% decomposition after 240 min. In general, sulfur activators are more efficient, especially at pH=8. The doped S element promotes the photo-Fenton reaction of S/$Fe_2O_3$ by two roles: retarding the recombination of photogenerated charge carriers and promoting the electron transfer between the peroxide species and iron ions at the interface [27].

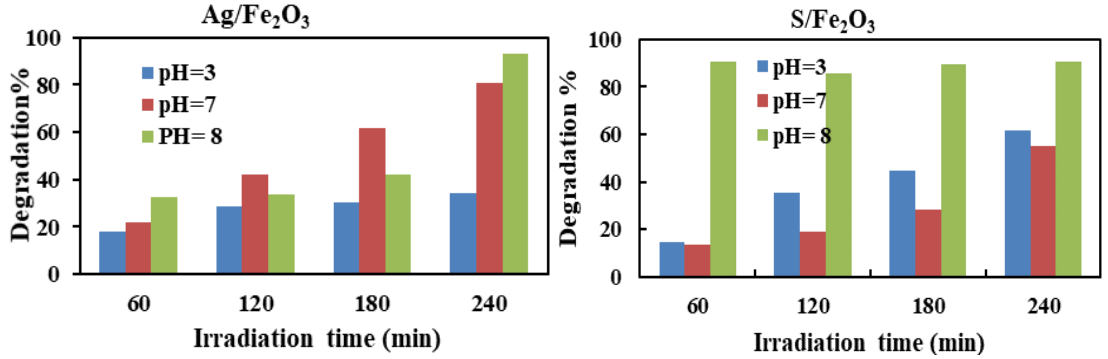


***Figure 5: Degradation percentage of MB(5ppm) by Ag/ $Fe_2O_3$ and S/$Fe_2O_3$ nanoparticles at pH=3 ,7 and 8 versus irradiation (0-240 min) time under solar light irradiation.***

Decomposition kinetics of MB dyes analysis were helpful in evaluating the photocatalytic activity of Ag/$Fe_2O_3$ and S/$Fe_2O_3$. The decomposition curves in Fig. 6 describe the change in absorbance (A) vs. irradiation time. Ln ($A_0$ /$A_t$) = kt was used to calculate the degradation rate constant for the decomposition process [25,26]. $A_0$ and $A_t$ are the starting and ultimate irradiation concentrations, respectively, and k is the pseudo-first-order rate constant. The rate constant values of Ag/$Fe_2O_3$ were 0.0076 $min^{-1}$, 0.006 $min^{-1}$ and 0.002 $min^{-1}$ at pH=8, pH= 7 and pH=3, respectively. S/$Fe_2O_3$ shows a greater rate constant values 0.0126 $min^{-1}$, 0.0021$min^{-1}$ and 0.0037 $min^{-1}$ at pH=8, pH=7 and pH=3, respectively, which means a higher photocatalytic activity.

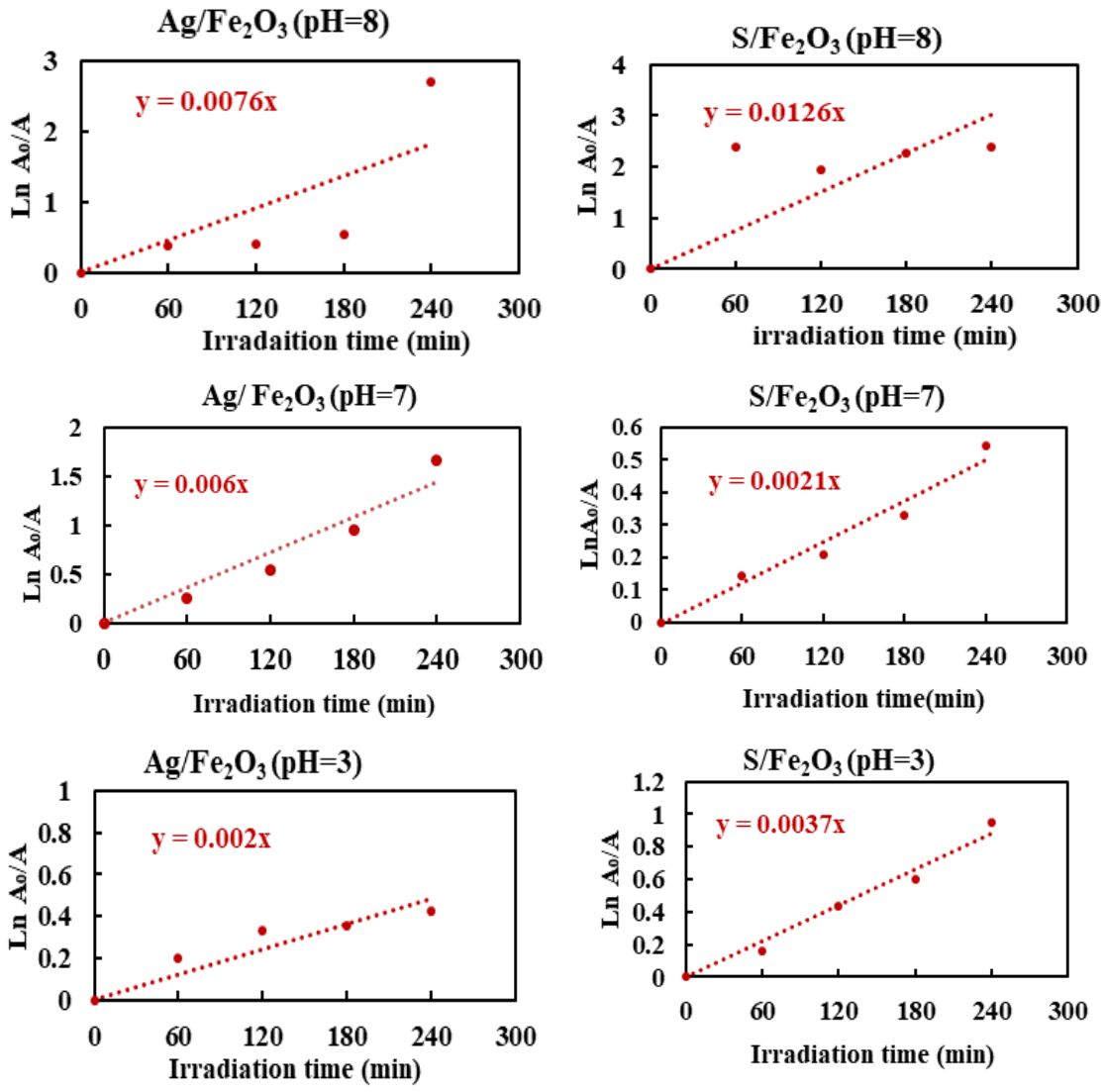


***Figure 6: Ln ($A_o/A_t$) vs. different irradiation times (0-240 min) for MB (5ppm) decomposition catalyzed by Ag/$Fe_2O_3$ and S/$Fe_2O_3$ under sunlight irradiation.***

## 4. Photocatalytic Mechanism

The process of MB dye degradation by $Fe_2O_3$ can be elucidated by a postulated mechanism as shown in Fig.7. When an $Fe_2O_3$ sample is exposed to sunlight, the energy from the sunlight causes electrons in the valence band (VB) to become excited and move to the conduction band (CB). This process also creates vacancies, or "holes," in the valence band. [28] Subsequently, the oxygen molecules present in the solution react with the available photoelectrons, resulting in the formation of free radicals. When water combines with holes, it forms ($^{\bullet}OH$), while ions can mix with oxygen to generate $^{\bullet}O^{-}_2$. When the MB dye attaches to the surface of $Fe_2O_3$, it undergoes a process called adsorption. During this process, free radicals ($^{\bullet}OH$) interact with the dye and cause it to break down into water ($H_2O$) and carbon dioxide ($CO_2$) [27].

$$Fe_2O_3 + \text{photon energy} \rightarrow e^{-}_{(CB)} + h^{+}_{(VB)}$$

$$e^{-}_{(CB)} + O_{2\,(ads)} \rightarrow {}^{\bullet}O^{-}_2$$

$$h^{+}_{(VB)} + H_2O_{\,(ads)} \rightarrow {}^{\bullet}OH$$

$^{\bullet}O^{-}_{2}$ + MB dye
→ degradation products
$^{\bullet}$OH +MB dye

$HO^{\bullet}$ + MB dye → Intermediate → $CO_2$ + $H_2O$

$Ag \rightarrow Ag^{+} + e^{-}_{(CB)}$

$Ag^{+} + e^{-}_{(CB)} \rightarrow Ag$

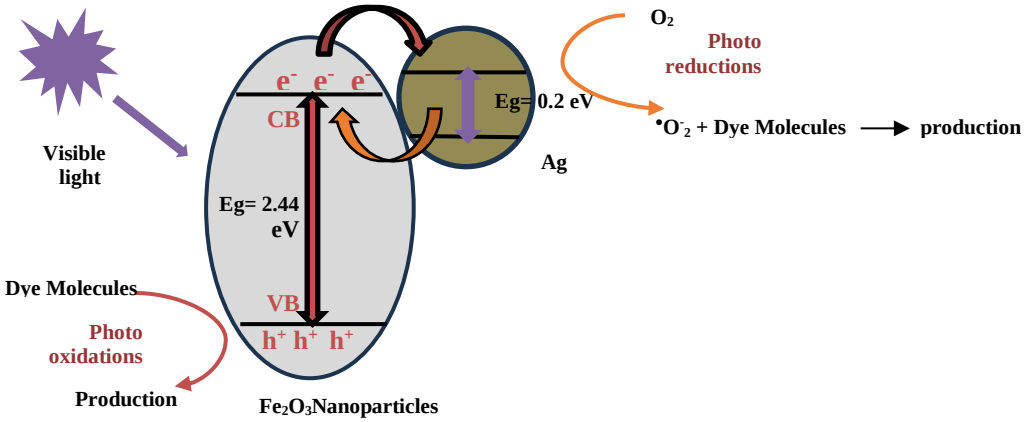


***Figure 7: Photocatalysis process by Ag/$Fe_2O_3$.***

The photocatalysis degradation by S/$Fe_2O_3$ is shown in Fig.8. The electrons captured by oxygen vacancies reduce $Fe^{3+}$ to $Fe^{2+}$. Then $Fe^{2+}$ reacts with $H_2O_2$ to produce OH with strong oxidation, which oxidizes dyes into $CO_2$ and $H_2O$.

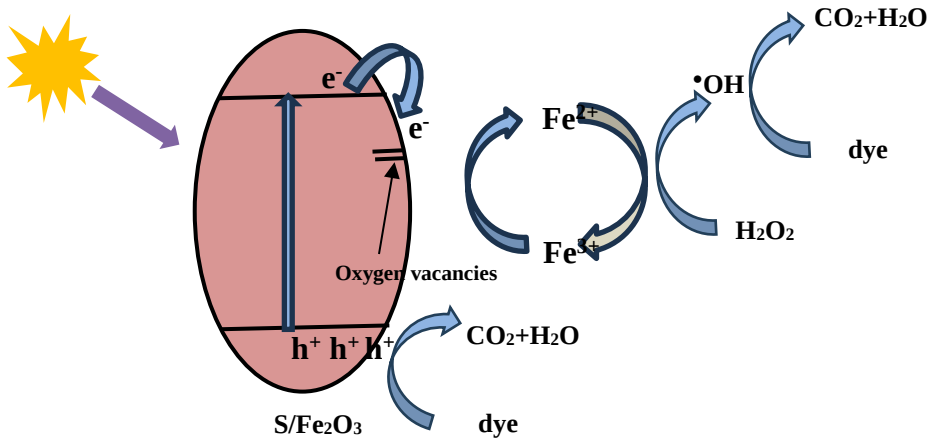


***Figure 8: Photocatalysis process by S/$Fe_2O_3$.***

## 5. Conclusions

This indicates that pH significantly affects the photocatalytic degradation performance of MB over Ag/$Fe_2O_3$ and S/S/$Fe_2O_3$ nanoparticles. Optimal degradation was found to be at alkaline values (pH = 8), achieving degradation efficiencies of up to 93.35% for S/S/$Fe_2O_3$ and 90% for Ag/Fe2O3 in the first 60 min of sunlight exposure. Such improved efficiency is ascribed to the enhanced hydroxyl radicals (•OH) yield in basic environments, facilitating effective photocatalytic reactions. Conversely, acidic

conditions (pH = 3) resulted in significantly lower degradation rates, highlighting the critical role of surface charge dynamics and hydroxyl radical availability. The sulfur-doped $Fe_2O_3$ is better than its silver counterparts because it enhances charge carrier dynamics and photo-Fenton oxidation reactions. This opens up possible environmental remediation using $Fe_2O_3$-based nanocomposite materials, such as in water treatment under optimised pH conditions. Future work might try to make this happen and test more dopants to find ways to enhance photocatalysis.

## Conflict of interest

Authors declare that they have no conflict of interest.

## References


1. S. S. Hashmi, M. Shah, W. Muhammad, A. Ahmad, M. A. Ullah, M. Nadeem, and B. H. Abbasi, J. Indian Chem. Soci. **98**, 100019 (2021). DOI: 10.1016/j.jics.2021.100019.
2. S. S. Vedula and G. D. Yadav, J. Indian Chem. Soci. **98**, 100017 (2021). DOI: 10.1016/j.jics.2021.100017.
3. S. Dey, P. Patra, and S. Pal, J. Indian Chem. Soci. **98**, 100066 (2021). DOI: 10.1016/j.jics.2021.100066.
4. A. S. Khalil, B. M. Al-Shabander, and H. M. Yaseen, AIP Conf. Proc. **2372**, 130019 (2021). DOI: 10.1063/5.0066068.
5. L. Xu, H. Suo, and R. Liu, J. Indian Chem. Soci. **98**, 100111 (2021). DOI: 10.1016/j.jics.2021.100111.
6. B. Alshabander and A.-A. Mays Bassim, Iraqi J. Phys. **21**, 10 (2023). DOI: 10.30723/ijp.v21i1.1042.
7. M. Sharif, A. Heidari, and A. Aghaeinejad, J. Photopoly. Sci. Tech. **32**, 27 (2019). DOI: 10.2494/photopolymer.32.27.
8. S. Zeng, K. Tang, T. Li, Z. Liang, D. Wang, Y. Wang, Y. Qi, and W. Zhou, J. Phys. Chem. C **112**, 4836 (2008). DOI: 10.1021/jp0768773.
9. X. Li, X. Yu, J. He, and Z. Xu, J. Phys. Chem. C **113**, 2837 (2009). DOI: 10.1021/jp8079217.
10. S. K. Mohapatra, S. E. John, S. Banerjee, and M. Misra, Chem. Mat. **21**, 3048 (2009). DOI: 10.1021/cm8030208.
11. Z. Liu, V. Subramania, and M. Misra, J. Phys. Chem. C **113**, 14028 (2009). DOI: 10.1021/jp903342s.
12. W. Luo, D. Wang, F. Wang, T. Liu, J. Cai, L. Zhang, and Y. Liu, Appl. Phys. Lett. **94**, 202507 (2009). DOI: 10.1063/1.3139780.
13. Suman, S. Chahal, A. Kumar, and P. Kumar, Crystals **10**, 273 (2020). DOI: 10.3390/cryst10040273.
14. A. Liu, C. Zhang, Y. Zhu, K. Li, J. Huang, Y. Du, and P. Yang, J. Coll. Interf. Sci. **535**, 408 (2019). DOI: 10.1016/j.jcis.2018.09.102.
15. H. Liu, K. Tian, J. Ning, Y. Zhong, Z. Zhang, and Y. Hu, ACS Cataly. **9**, 1211 (2019). DOI: 10.1021/acscatal.8b03819.
16. Y. Zhang, S. Jiang, W. Song, P. Zhou, H. Ji, W. Ma, W. Hao, C. Chen, and J. Zhao, Ener. Envir. Sci. **8**, 1231 (2015). DOI: 10.1039/C4EE03803G.
17. L. Guo, F. Chen, X. Fan, W. Cai, and J. Zhang, Appl. Cataly. B Envir. **96**, 162 (2010). DOI: 10.1016/j.apcatb.2010.02.015.
18. G. K. Pradhan, N. Sahu, and K. M. Parida, RSC Adv. **3**, 7912 (2013). DOI: 10.1039/C3RA23088K.
19. D. Wu and Z. Zhang, Electrochim. Acta **282**, 48 (2018). DOI: 10.1016/j.electacta.2018.06.045.
20. E. Mccafferty, Electrochim. Acta **55**, 1630 (2010). DOI: 10.1016/j.electacta.2009.10.040.
21. X. Li, Y. Hou, Q. Zhao, and L. Wang, J. Coll. Interf. Sci. **358**, 102 (2011). DOI: 10.1016/j.jcis.2011.02.052.
22. I. Kazeminezhad and A. Sadollahkhani, J. Mat. Sci: Mat. Electron. **27**, 4206 (2016). DOI: 10.1007/s10854-016-4284-0.
23. B. Neppolian, S. Sakthivel, B. Arabindoo, M. Palanichamy, and V. Murugesan, J. Envir. Sci. Heal. Part A **34**, 1829 (1999). DOI: 10.1080/10934529909376931.
24. L. Jayarathna, A. Bandara, W. J. Ng, and R. Weerasooriya, J. Envir. Heal. Sci. Eng. **13**, 54 (2015). DOI: 10.1186/s40201-015-0210-2.
25. K. Bhuvaneswari, G. Palanisamy, G. Bharathi, T. Pazhanivel, I. R. Upadhyaya, M. L. A. Kumari, R. P. Rajesh, M. Govindasamy, A. Ghfar, and N. H. Al-Shaalan, Envir. Res. **197**, 111079 (2021). DOI: 10.1016/j.envres.2021.111079.

26. G. Palanisamy, K. Bhuvaneswari, A. Chinnadurai, G. Bharathi, and T. Pazhanivel, J. Phys. Chem. Sol. **138**, 109231 (2020). DOI: 10.1016/j.jpcs.2019.109231.
27. A.-L. Safaa Ahmed and A.-S. Ban Mazin, Iraqi J. Phys. **20**, 54 (2022). DOI: 10.30723/ijp.v20i4.1051.

# تأثير pH على فعالية التحفيز الضوئي للجسيمات النانوية $S\backslash Fe_2O_3$ و $Ag/Fe_2O_3$ بواسطة تحلل صبغة الميثيل الزرقاء

**براء عقيل كريم[1] وبان مازن الشابندر[1]**
*لقسم الفيزياء، كلية العلوم، جامعة بغداد، بغداد، العراق*

## الخلاصة

تم إنتاج جسيمات نانوية من أكسيد الحديد ($Fe_2O_3$) المطعم ب 5% mol من المواد المعدنية الفضة (Ag) والمواد غير المعدنية الكبريت(S)، وباستخدام عملية التلقيح المائية . تم استخدام المجهر الالكتروني الماسح (SEM) لتحديد شكل وترتيب البلورات. تم استخدام مطياف UV-visلدراسة التحلل الضوئي لملوثات الصبغة عن طريق قياس أطياف الامتصاص لعينات $Ag/Fe_2O_3$ و $S/Fe_2O_3$. كان الهدف من هذه الدراسة هو دراسة تأثير الاس الهيدروجيني على فعالية التحفيز الضوئي للجسيمات النانوية. تم تغيير الرقم الهيدروجيني لمحلول من صبغة أزرق الميثيلين (MB) بتركيز 5 ppm إلى 3 و 8 باستخدام حمض الهيدروكلوريك (HCl) وهيدروكسيد الصوديوم (NaOH). عند pH = 8، يستغرق $Ag/Fe_2O_3$ حوالي 240 دقيقة ليصل إلى ما يقرب من 93.35% من التحلل، بينما يحقق $S/Fe_2O_3$ أكثر من 90% من التحلل في أول 60 دقيقة من عملية التحفيز الضوئي. عند pH = 3، يحقق $Ag/Fe_2O_3$ فقط 34.46%، بينما يحقق $S/Fe_2O_3$أكثر من 61.44% من التحلل بعد 240 دقيقة من عملية التحفيز الضوئي. لقد وجد ان طريقة pseudo first order kinetic مناسبة لامتصاص صبغة (MB) بواسطة المحفزين.

**الكلمات المفتاحية:** $Fe_2O_3$، التحفيز الضوئي، المثيل الازرق، الصبغة، التحلل.